ADVANCED FUNCTIONAL MATERIALS
www.afm-journal.de

3D-Printable Shape-Memory Polymers Based on Halogen Bond Interactions

*Josefine Meurer, Robin H. Kampes, Thomas Bätz, Julian Hniopek, Oswald Müschke, Julian Kimmig, Stefan Zechel, Michael Schmitt, Jürgen Popp, Martin D. Hager, and Ulrich S. Schubert**

The supramolecular halogen bonding (XB) is utilized for the first time for the preparation of shape-memory polymers. For this purpose, an iodotriazole-based bidentate XB donor featuring a methacrylamide is synthesized. Free radical polymerization of the XB donor monomer together with butyl methacrylate, triethylene glycole dimethacrylate, and methacrylic acid results in covalently cross-linked polymer networks bearing both, halogen bond acceptors and donors, in their side chains. While the reversible halogen bond interactions can act as switching unit, the required stable phase of the shape-memory polymers is formed by covalent cross-links. The successful formation of the supramolecular cross-links is proven via Fourier-transform Raman spectroscopy. Furthermore, the thermal properties are investigated via differential scanning calorimetry and thermo gravimetric analysis. Thermo-mechanical analysis reveals excellent shape-memory abilities with fixity rates above 95% and recovery rates up to 99%. Moreover, it is possible to 3D-print this kind of material exhibiting the ability to recover its shape within a few seconds at 130 °C.

1. Introduction

The halogen bond (XB) is a supramolecular interaction between a Lewis base (XB acceptor) and a Lewis acid (XB donor).[1] The XB is very directional and enables precise tuning of the interaction strength by the choice of the halogen atom and the polarization strength of the substituent. Additionally, the XB features another advantage in terms of lower hydrophilicity compared to the familiar hydrogen bond enabling the application in aqueous environments.[2,3] The XB is well established in chemistry and, in particular, in research fields like anion recognition and sensing,[4,5] crystal engineering,[6] and organo-catalysis.[7,8] In contrast, the halogen bond is still underrepresented in polymer and material science. Considering the very successful utilization of hydrogen bonds for stimuli-responsive materials, also XB is getting more and more popular in stimuli-responsive polymers (e.g., self-healing polymers[9,10]), since it offers great benefits such as high directionality of the bond and higher stability against water or moisture.[11]

One interesting class of such intelligent materials are shape-memory polymers (SMP).[12–16] Such polymers have the unique ability to "memorize" their original (permanent) shape after they have been converted into a completely new (temporary) shape under certain conditions.[17–20] Hereby, the complete structure of the polymer is responsible for the ability to reveal shape-memory properties and not just one specific unit.[12–15] In general, it requires two different building parts to design a SMP – the stable phase and the switching unit. With the help of the stable phase, the complete polymeric system gains stability and the deformation of these units also results in the driving force for the recovery step. Herein, in most cases physical[21] or covalent cross-linking[19,22] is applied. The second building part must be addressable with the desired trigger and is called switching unit. The most

J. Meurer, R. H. Kampes, T. Bätz, O. Müschke, J. Kimmig, S. Zechel, M. D. Hager, U. S. Schubert
Laboratory of Organic and Macromolecular Chemistry (IOMC)
Friedrich Schiller University Jena
Humboldstr 10, 07743 Jena, Germany
E-mail: ulrich.schubert@uni-jena.de

The ORCID identification number(s) for the author(s) of this article can be found under https://doi.org/10.1002/adfm.202207313.

DOI: 10.1002/adfm.202207313

J. Meurer, R. H. Kampes, T. Bätz, O. Müschke, J. Kimmig, S. Zechel, J. Popp, M. D. Hager, U. S. Schubert
Jena Center for Soft Matter (JCSM)
Friedrich Schiller University Jena
Philosophenweg 7, 07743 Jena, Germany

J. Hniopek, M. Schmitt, J. Popp
Institute of Physical Chemistry (IPC)
Friedrich Schiller University Jena
Helmholtzweg 4, 07743 Jena, Germany

J. Hniopek, M. Schmitt, J. Popp, U. S. Schubert
Abbe Center of Photonics (ACP)
Friedrich Schiller University Jena
Albert-Einstein-Straße 6, 07745 Jena, Germany

J. Hniopek, J. Popp
Department Spectroscopy & Imaging
Leibniz Institute of Photonic Technology (IPHT) e. V. Jena
Albert-Einstein-Straße 9, 07745 Jena, Germany

common way is the use of a thermal transition like the glass transition[23] or those between crystallization and melting.[22] However, it has already been shown that reversible bonds, covalent[24] or supramolecular[25] in nature, can represent very suitable switching units. In the field of supramolecular bonds as the switching unit, there are already various examples using hydrogen bonds,[18,26] ionic interactions,[27,28] or reversible metal complexes,[29,30] respectively. However, the aforementioned promising XB interaction has, to the best of our knowledge, not been utilized so far for the design of shape-memory polymers.

The motivation of this study is the combination of covalent cross-linking for the stable phase simultaneous with halogen bond interaction based reversible cross-linking for the switching unit. These reversible supramolecular interactions can be activated at elevated temperatures and, therefore, act as switching units in this new kind of shape-memory polymers.

2. Results and Discussion

2.1. Synthesis of the Polymers

For the synthesis of shape-memory polymers based on reversible XB interactions, first, a methacrylamide monomer bearing a halogen bond donor (**XB-MA**) was synthesized (for detailed information see the Supporting Information). The binding behavior and the experimental and theoretical analysis of the halogen bonds formed by such a XB-donor were previously studied in solution.[31,32] However, the XB donor motif has not been transferred into supramolecular materials yet. For this purpose, a carbazole was functionalized with two iodotriazole moieties enabling a bidentate complexation of a XB acceptor. Furthermore, the XB donor features a polymerizable group via a methacrylamide functionality. The donor's suitability to form a halogen bond with carboxylic acid or carboxylates was approved with isothermal titration calorimetry using acetic acid or tetrabutylammonium acetate as XB acceptors (for detailed information see Figures S12 and S13, Supporting Information) revealing a relatively weak and, thus, addressable supramolecular bond.

Afterwards, all polymer networks were synthesized via free radical polymerization using the synthesized **XB-MA** monomer, butyl methacrylate (BMA) as main monomer, triethylene glycol dimethacrylate (TEGDMA) as covalent crosslinker and methacrylic acid (MAA) as XB acceptor (see **Figure 1**a). To investigate the structure-property-relationship, the content of the **XB-MA** and MAA as well as the TEGDMA was varied (see **Table 1**). For the synthesis of **P1** and **P2**, 5% of the TEGDMA crosslinker was utilized, while it was omitted for the polymerization of **P3**. Furthermore, 5% of **XB-MA** and MAA were utilized in case of **P1** and **P3** and on the other hand, 10% of each for **P2**. For this reason, **P1** and **P2** resulted in covalently and supramolecular crosslinked, insoluble polymer networks, while **P2** exhibits a significantly higher supramolecular crosslinking density compared to **P1**. In contrast, **P3** just contains the supramolecular XB-cross-linking featuring (low) solubility.

Since carboxylates are far better XB acceptors (i.e., Lewis bases) compared to the carboxylic acids,[33] furthermore, ionic polymer networks **P1-I** to **P3-I** were synthesized via deprotonation of the polymers **P1** to **P3** (see Figure 1b) with tetra-butyl ammonium hydroxide solution. All polymers were afterwards characterized using elemental analysis. It could be revealed that in all polymers the XB donor moiety could be incorporated due to the found iodine content. Furthermore, the increased nitrogen and the reduced carbon content in case of **P2** indicates a higher amount of XB-donor, which goes hand in hand with the synthetic approach using the double amount of XB-monomer for the preparation of **P2**. A similar observation could also be made for the ionic polymers **P1-I** to **P3-I**, in which a higher iodine content of 9.9% was found for **P2-I** (compared to 6.5% for **P1-I**) revealing also a higher XB-donor content for the ionic polymers. Furthermore, the solubility of **P3** due to the lack of a covalent crosslinker made it possible to calculate its exact composition via ^{1}H NMR spectroscopy. Here, an **XB-MA** content of 6.25% was calculated, which comes very close to the 5% utilized and also fits together with the results of the elemental analysis. Further detailed information for the synthesis and characterization of all polymers is presented in the Supporting Information.

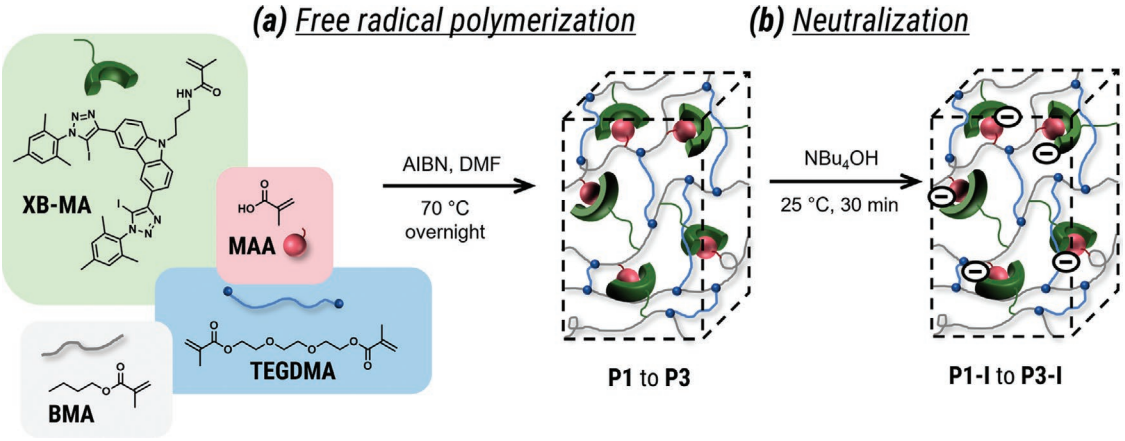

Figure 1. a) Schematic representation of the synthesis of the halogen bond based polymer networks **P1** to **P3** via free radical polymerization and b) ionic polymer networks **P1-I** to **P3-I** via the addition of tetra-butyl ammonium hydroxide (NBu_4OH).

Table 1. Utilized quantities of the monomers for the synthesis of the polymer networks via free radical polymerization.

Polymer	Composition (utilized for synthesis)		
	XB-MA content [%]	MAA content [%]	TEGDMA content [%]
P1 **P1-I**	5.0	5.0	5.0
P2 **P2-I**	10.0	10.0	5.0
P3 **P3-I**	5.0	5.0	–

2.2. Raman Spectroscopic Investigation

To investigate the molecular structure of the polymers and to specifically confirm the formation of halogen bonds in the polymers, all samples were investigated using Fourier-transform (FT) Raman spectroscopy at 1064 nm excitation wavelength. All FT-Raman measurements were performed with samples in the solid state. Raman spectroscopy represents an established method to visualize the formation of halogen bonds.[9,34,35] Due to its noninvasive nature and the lack of necessary sample preparation, it can be applied directly to the polymer environment in its solid state without requiring solvents. For this reason, it is an ideal tool to establish the halogen bond based cross-linking inside the polymer networks.[9,10]

The formation of a halogen bond involves a charge-transfer leading to a partial population of σ^*(C-X) orbitals and a characteristic weakening and lengthening of the C—X bond.[35,36] This behavior can be detected by a shift of the band for the C—X stretching vibration to lower wavenumbers.[34] Indeed, this characteristic shift of the C—I stretching band located at 283 cm^{-1} in free **XB-MA** to lower wavenumbers (see the detailed band assignment in the Supporting Information), can be observed for all ionic polymers **P1-I** to **P3-I** (see **Figure 2**a). By fitting Voigt profiles to the bands (further details see in the Supporting Information), a redshift of 6–8 cm^{-1} can be determined for all three polymers indicating similar binding conditions for all polymers. Furthermore, the formation of the halogen bonds in the case of **XB-MA** induces changes in the electronic structure of the triazolium and further conjugated moieties underlying the formation of the halogen bond.[9] For all ionic polymers (**P1-I** to **P3-I**), changes for aromatic stretching vibrations between 1530 and 1610 cm^{-1} can be observed (see Figure 2a). These results clearly indicate the formation of halogen bonds inside the ionic polymer networks.

For the non-ionic polymers **P1** to **P3**, only very small (≈1 cm^{-1}) shifts of the C—I band position could be observed (see Figure 2b). Since the magnitude of the shift is directly related to the strength of the halogen bond, this finding indicates that the halogen bond network inside the non-ionic polymers is comparatively very weak – an expected observation, as the strength of halogen bonds is significantly strengthened by charged acceptor molecules.[37] The same observation could be found for the aromatic vibrations (see Figure 2b), indicating the presence of only very weak halogen bonds in the non-ionic polymer networks **P1** to **P3**. A detailed comparison of the characteristic signals is presented in Table S9 (Supporting Information). In addition to those findings, FT-Raman spectroscopy was utilized to prove that the samples prepared do not contain any residual solvent or unpolymerized double bonds (see Figures S70 and S71, Supporting Information).

2.3. Investigation of the Thermal Properties

The thermal properties represent a key parameter in the field of thermally induced shape-memory materials. A detailed description of these investigations is presented in Figures S19–S33 and Tables S2 and S4 (Supporting Information). First, the thermal stability plays a very important role since a switching temperature, at which the sample is not damaged, has to be selected. To determine the degradation temperature (T_d) of the polymer networks (**P1** to **P3** and **P1-I** to **P3-I**) thermo-gravimetric analyses (TGA) were performed. The measurements revealed T_d-values above 180 °C for all samples (see Figure 2c). Within the TGA-curves, in particular for the samples **P1** to **P3**, a stepwise mass loss at a temperature of 200 °C was observable, which presumably was caused by the decomposition of the iodine-bond in the utilized **XB-MA**. On the one hand, this assumption is supported by the fact that the mass loss in case of **P1** and **P3** (containing ≈5% **XB-MA**) is extremely similar, while a significantly higher mass loss was observed in the case of **P2** (containing ≈10% **XB-MA**) at 200 °C. Furthermore, a similar thermal behavior was already reported in literature for polymers containing comparable XB-donor functions in their side-chains.[9] It was further found that the degradation temperature of the ionic polymer networks **P1-I** to **P3-I** is in general lower compared to the polymer networks **P1** to **P3** (see Figures S28–S32, Supporting Information for a comparison of ionic and non-ionic polymers). This presumably results from the prior degradation of the tetra-butyl ammonium, which remains as counter ion in the polymer after the neutralization step and is sensitive to lower temperatures.

The next important value is the glass transition temperature (T_g), as it provides information about the temperature, at which deformation of the polymer is in principle possible. To measure T_g, differential scanning calorimetry (DSC) measurements were performed for all polymers. The DSC measurements revealed glass transition temperatures below 100 °C for all investigated polymers (see Figure 2d). In general, the glass transition temperature of the six different polymers is influenced by several molecular parameters, including the amount of covalent cross-linker, the type and strength of the supramolecular interaction as well as the amount of halogen bonds within the polymer. Furthermore, in case of the ionic XB-acceptor, additional ionic interactions are possibly leading to further supramolecular bindings and the formation of clusters as known for ionic polymers[38] resulting in an increase of the glass transition temperature. In contrast, the introduction of large counter ions, i.e., tetra-butyl ammonium, could also lead to a decrease of the T_g-value of the ionic polymers compared to their neutral analogs, as also known for ionic polymers.[39]

Thus, the observed glass transition temperatures of the different polymers can be explained by the interplay of all these influencing parameters. It was found that the polymers **P1** and **P1-I** exhibit lower T_g-values compared to **P2** and **P2-I**,

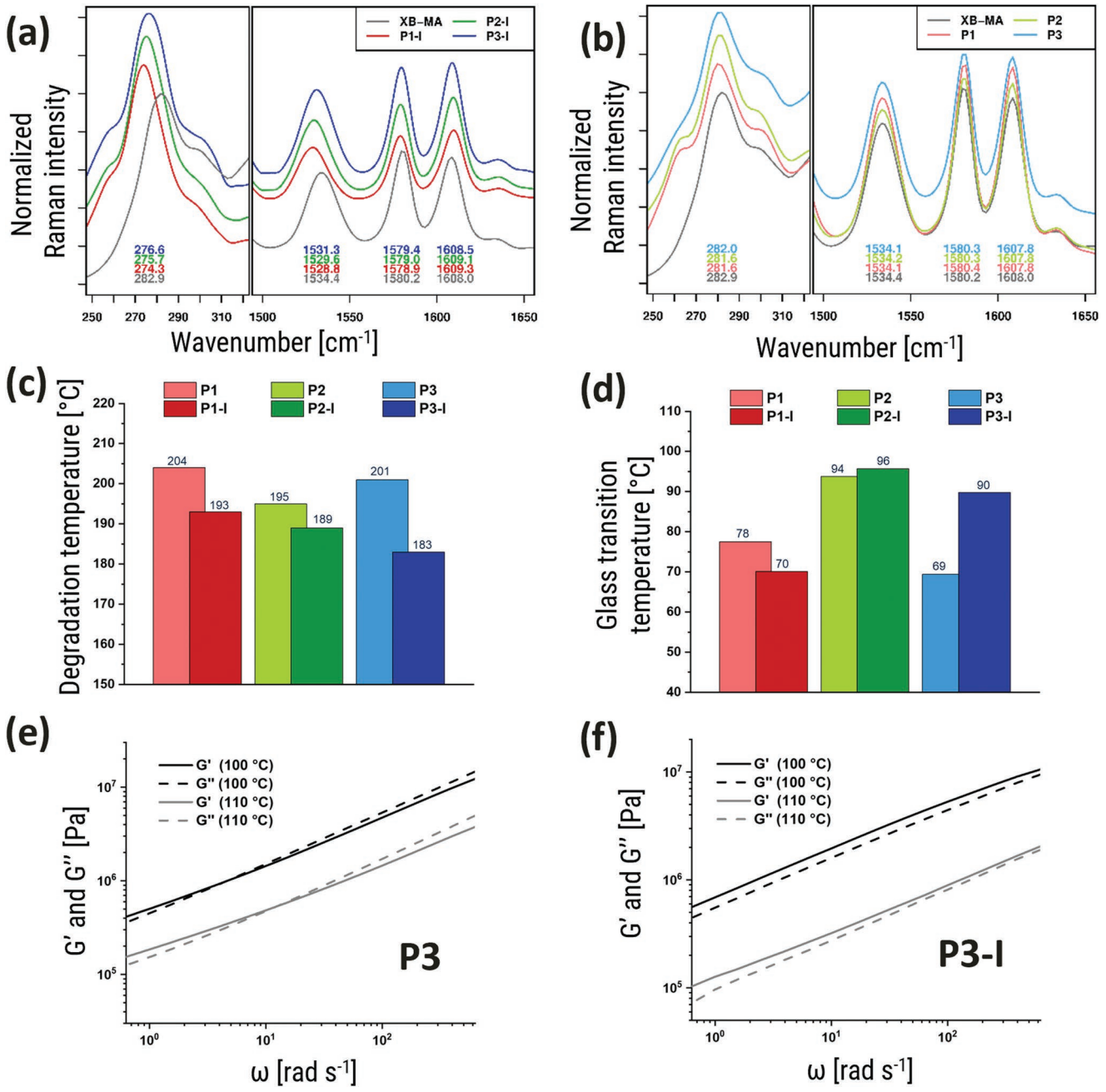

Figure 2. FT-Raman spectra of **XB-MA** and a) the ionic polymer networks **P1-I** to **P3-I** and b) the carboxylic acid containing polymer networks **P1** to **P3**. c) Comparison of the determined degradation and d) glass transition temperatures of all polymers. Results of the frequency sweep measurements at 100 and 110 °C for the polymers e) **P3** and f) **P3-I**.

presumably resulting from the different supramolecular cross-linking density. **P3** also revealed a lower T_g-value compared to **P1** and **P2** due to the missing covalent cross-linker. The DSC curves of all samples are displayed in Figures S19–S27 (Supporting Information).

Additionally, an influence of the ionic character and, thus, the increase in binding strength and additional ionic interactions could be determined. This behavior was most noticeable for **P3** and **P3-I**. The investigation revealed a glass transition temperature of 69 °C for **P3**, while its ionic version **P3-I** exhibits a T_g 20 K higher (90 °C). The polymers **P2** and **P2-I** showed the same behavior to a lower extend. In contrast, **P1** and **P1-I** revealed an inverse behavior presumably due to a "softener" effect of the bulky counter ion; however, both T_g-values (of **P1** and **P1-I**) are comparable to each other. Furthermore, temperature dependent dynamic-mechanical-analyses (DMTA) confirmed the results of the DSC investigations for the covalently cross-linked polymer networks (see Tables S2 and S4, Supporting Information). Samples **P1** and **P1-I** already softened at ≈70 °C, whereas samples **P2** and **P2-I**, containing roughly

double the proportion of halogen bonds, only showed a reduction in mechanical properties at higher temperatures (≈90 °C). The resulting DMTA plots are displayed in Figures S34–S37 (Supporting Information).

To investigate the stability and the possibility to activate the halogen bond interaction, frequency sweep experiments at 100 and 110 °C were carried out with the polymers **P3** and **P3-I** (Figures S38 and S39, Supporting Information). The application of this method was found to be a suitable strategy to study the addressability of supramolecular interactions in the solid state at different temperatures.[40,41] In case of a reversible supramolecular interaction, a crossover of the storage (G') and loss modulus (G'') can be detected.[40,41] Consequently, it is also possible to calculate the supramolecular bond lifetime (see Equation S1, Supporting Information).[40] These investigations revealed significant differences in the reversible character of the halogen bond based on the acid (**P3**) or the carboxylate (**P3-I**) as XB acceptor. **P3** features a crossover of G' and G'' during the frequency sweep investigations at both temperatures. Whereas at 110 °C, a supramolecular bond lifetime of 0.47 s could be measured, at 100 °C the lifetime was found to be 1.40 s. These results indicate a suitable thermal activatability of the halogen bonds formed between the halogen bond donors and the acid groups. In contrast, during the frequency sweep investigations of **P3-I** the slopes of G'' and G' come very close at very high frequencies; however, no crossover could be detected. This finding indicates a very slow activation of the halogen bonds in the ionic networks, since a very high supramolecular bond lifetime can be assumed due to the convergence of G'' and G'.

2.4. Investigation of the Shape-Memory Abilities

The intention of this study was the investigation of the shape-memory abilities featured by new halogen bond based materials. For this reason, a permanent shape was determined via hot-pressing (150 °C) resulting in rectangular polymer rods (see **Figure 3**a). All fabricated samples revealed shape-memory abilities during a manual test at 115 °C. A photo series of the shape-memory test for the sample **P2** and a schematic representation of the shape-memory process are presented in Figure 3a. The photo series of the remaining samples are displayed in Figure S53 (Supporting Information). The shape-memory cycle starts with the polymer in its permanent shape, in which all chains are in their relaxed state. Heating the polymer activates the reversible supramolecular cross-links. The deformation at this temperature leads to a tightening of the chains; however, the polymer network is still fixed by the covalent cross-linker. Holding the polymer in its shape during cooling below the switching temperature deactivates the reversible halogen bonds and the regained supramolecular cross-linking prevents the stressed polymer chains from rearranging into the relaxed form. Consequently, the polymer is fixed in the temporary shape. For the recovery step, the halogen bonds are again activated by heating, allowing the chains to relax again under stress free condition and to recover the permanent shape.

For the polymers **P3** and **P3-I,** this mechanism must be slightly different, as those two polymers do not contain a covalent cross-linker; however, both polymers still exhibit excellent shape-memory abilities. We assume that the halogen bond interaction is reversible due to exchange reactions (or the reversible formation of clusters, see discussion below for a potential mechanism) between different moieties, which was also reported recently.[42] Thus, the halogen bonds act as switching unit and stable phase simultaneously, enabling shape-memory behavior without any further irreversible cross-linking.

In general, there are two major routes, through which the halogen bond enables the shape-recovery behavior of the materials. On the one hand, there is the possibility of exchange reactions of the two different halogen bond moieties, as known for several reversible covalently[43] or supramolecularly[44,45] cross-linked polymers. In contrast, the high activation temperature of the rather weak supramolecular bond could, however, also indicate the formation of clusters consisting of multiple halogen bond moieties. Such clusters have been described for structurally related hydrogen bonds[46,47] or ionic polymers,[48] in particular for relatively non-polar polymer backbones.[49,50] These clusters lead to far stronger supramolecular bonds in the solid state compared to the complex association constant of the bond motif in solution would have suggested.[46,47] Nevertheless, the utilized halogen bond, which was previously shown to be relatively weak (see ITC and Raman results), can only be switched at temperatures above 100 °C potentially indicates the formation of such higher ordered structures.

Due to the structural design of the materials, the reversible behavior of the investigated polymers could in principle also be based on hydrogen bonds, e.g., between the methacrylic acid units via dimer formation. In order to exclude this interaction as potential predominant mechanism for the shape-memory behavior, a control experiment was performed. For this purpose, the polymer **P(BMA-*co*-MAA)** containing 11% carboxylic acid side chains was prepared (for details see the Supporting Information). However, no shape-memory properties could be observed in a manual test of this sample revealing that the XB is the major reversible interaction required for the shape-memory behavior observed for these materials. A detailed discussion for this investigation as well as a photo series of the manual shape-memory test is presented in (see Figure S16, Supporting Information). These findings also go hand in hand with a study of Lewis et al., in which the authors investigated how the shape-memory process is influenced by hydrogen bonds of different strength.[51] As part of this study, the authors were able to show that weaker hydrogen bonds (e.g., carboxylic acids) have no significant effect on the shape memory properties of the polymers. The polymers containing these weak supramolecular bonds showed the shape-memory effect, but this was independent of the hydrogen bonds used and was only determined by the T_g of the polymeric network. Only the utilization of ureidopyrimidone (upy) side chains, which form significantly stronger hydrogen bonds compared to MAA units, enabled switching at significantly higher temperatures via these reversible groups.[51]

To investigate the shape-memory process in more detail and to quantify the shape-memory abilities of all samples, thermo mechanical analysis (TMA) was performed. With this methodology, it is possible to calculate the strain fixity (R_f) and the strain recovery rate (R_f) (Equations 1 and 2). The strain fixity rate quantifies the ability of a polymer to fix a mechanical deformation, while the strain recovery rate shows the efficiency

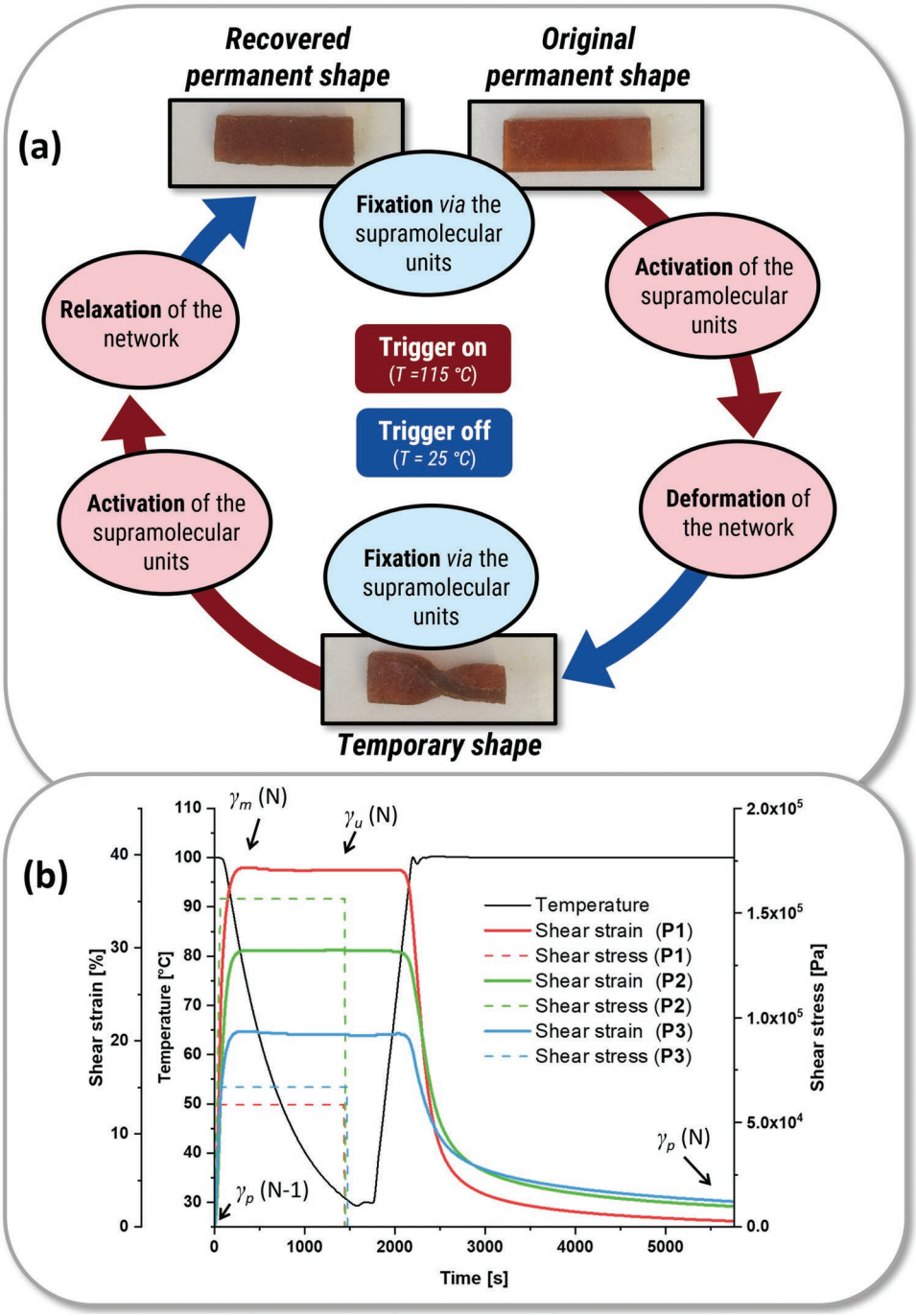

Figure 3. a) Photo series of the shape-memory behavior of **P2** (samples size about 3 cm × 0.3 cm × 1 cm) and schematic representation of the proposed underlaying mechanism within the polymer networks featuring halogen bond interactions as switching unit. b) TMA plots (2nd cycle) of the polymer networks **P1** to **P3** at a switching temperature of 100 °C.

of the regeneration of the original shape. Exemplarily the resulting TMA plots of **P1** to **P3** at a switching temperature of 100 °C are displayed in Figure 3b (see additional information in Figures S40–S52 and Table S5, Supporting Information). The TMA measurements also indicate that the switching of the polymers is presumably achieved via the supramolecular interactions. Regardless of their composition and glass transition temperature, all polymers switch at ≈100 °C.

This behavior can be seen in the very similar curves displayed in Figure 3b. The polymers **P1** and **P3** for example, exhibit a T_g of ≈70 °C. If the presented systems would switch based on their glass transition, like it is known for other systems,[23,28] and as it is described for systems that bear hydrogen bonds which are too weak,[51] a recovery process should already be observed at much lower temperatures (<<100 °C). The fact that in the samples we present, the recovery step does not take place as soon

as the T_g of the polymer network is reached, speaks strongly for switching via the reversible XB interactions. The comparison plots for **P1-I** to **P3-I** are shown in Figure S50 (Supporting Information). These materials feature again a similar behavior – the switching is independent from the T_g of the materials.

$$R_f(N) = \frac{\gamma_u(N)}{\gamma_m(N)} \times 100\% \quad (1)$$

$$R_r(N) = \frac{\gamma_m(N) - \gamma_p(N)}{\gamma_m(N) - \gamma_p(N-1)} \times 100\% \quad (2)$$

All calculated values of the strain recovery and fixity rate are summarized in **Table 2**. The measurements revealed excellent shape-memory abilities for all polymers. All determined strain fixity rates are above 95%. The best shape-memory performance was found for **P1** and **P1-I**. Those two polymers reveal recovery and fixity rates close to 100% already at a switching temperature of 100 °C. In comparison, the polymers **P2** and **P2-I** exhibit a slightly reduced recovery potential at 100 °C (80–90%).

For this reason, the measurements were repeated at a switching temperature of 110 °C further increasing the recovery rates in general above 96%. The polymer **P3**, lacking a covalent cross-linker, also revealed lower recovery rates (86–90%) at 100 °C compared to **P1**, which has otherwise the same composition. Raising the switching temperature to 110 °C led to a lowering of the obtained recovery rates, in contrast to the behavior of **P2** and **P2-I**. As discussed above, in the case of **P3** the halogen bond interaction presumably acts as switching unit and stable phase at the same time. An increase of the temperature may activate the supramolecular interaction more intensively resulting in a partial rewriting of the stable phase. Furthermore, it was found that the ionic polymers (**P1-I** to **P3-I**) revealed the restoration of the original shape with an even slightly higher recovery rate compared to the non-ionic polymers.

2.5. 3D-Printing

The 3D-printing of polymers and, in particular, of SMPs gets more and more popular based on the ability to obtain defined and individualized 3D-shapes applying a rather simple processing method.[52–55] As the last part of this study, it was investigated whether it is possible to 3D-print this type of shape-memory polymers, further named $\mathbf{P_{3D}}$ (see **Figure 4**). For this reason, a mixture of the four monomers was prepared. Again, BMA was utilized as main monomer. The content of the covalent cross-linker was raised to 15%, which is a well-suited ratio for the 3D-printing of this kind of monomer mixture. The content of the MAA and **XB-MA** had to be reduced to 2.5% due to the moderate solubility of the **XB-MA** in BMA. Furthermore, phenyl-*bis*-(2,4,6-trimethylbenzoyl)-phosphine oxide (BAPO) was added as a suitable photo-initiator at the wavelength of the 3D-printer, (detailed information can be seen in the Supporting Information).[56] The monomer mixture was filled into the 3D-printer (see Figure 4a). With the layer-by-layer photopolymerization of the monomers, it was possible to obtain the spiral-shaped polymer specimen $\mathbf{P_{3D}}$ (see Figure 4b). The complete polymerization of all double bonds could be confirmed via FT-Raman spectroscopy (see Figure S71, Supporting Information). At a switching temperature of 130 °C, a completely new temporary shape could be fixed (see Figure 4c), in which the sample stayed until it was again heated to 130 °C, inducing the regeneration of the originally printed, planar spiral-shape (see Figure 4d) within a few seconds. Since $\mathbf{P_{3D}}$ contains a significantly higher proportion of covalent cross-linker and, therefore, is slightly brittle, it was required to increase the switching temperature to 130 °C in order to ensure that the sample would not be damaged during the manual shape-memory test. It was also possible to repeat this several times without any apparent deterioration of the sample, depicted in a photo series in Figure S57 (Supporting Information). Furthermore, it was also possible to print a more complex model (see Figure 4e), which also revealed good shape-memory abilities. For this purpose, a butterfly was printed, whose wings were deformed during the shape-memory analysis, and the recovery of the permanent printed shape could be observed. Additionally, photos of a even more complex 3D-printed pyramid are displayed in (Figure S58, Supporting Information).

The 3D-printed polymer was also analyzed in a detailed fashion (see Figures S54–S53, Supporting Information). The formation of the halogen bond could be proven by FT-Raman spectroscopy (for a detailed discussion and the corresponding spectrum, see the Supporting Information). A glass transition

Table 2. Calculated fixity and recovery rates for the polymer networks **P1** to **P3** and **P1-I** to **P3-I**.

Polymer	T_{sw} [°C]	Strain fixity rate R_f [%]				Strain recovery rate R_r [%]			
		1st	2nd	3rd	4th	1st	2nd	3rd	4th
P1	100	99.6	99.5	99.2	98.9	95.2	98.4	98.9	99.1
P2	100	99.8	99.7	99.6	99.6	82.7	92.6	94.9	95.9
	110	99.9	99.9	99.9	99.8	93.9	96.6	97.2	97.7
P3	100	98.4	98.1	98.4	97.6	86.7	87.1	88.7	90.0
	110	98.5	98.3	98.6	98.5	81.2	83.1	86.0	87.5
P1-I	100	98.9	98.8	98.8	98.8	98.6	99.3	99.5	99.5
P2-I	100	99.6	99.5	99.5	99.4	83.9	98.8	92.4	94.2
	110	99.7	99.6	99.6	99.6	92.8	96.6	97.8	98.1
P3-I	100	97.4	96.8	96.4	95.7	88.3	94.0	95.4	96.8
	110	97.5	97.4	97.0	96.9	97.9	95.2	96.2	96.5

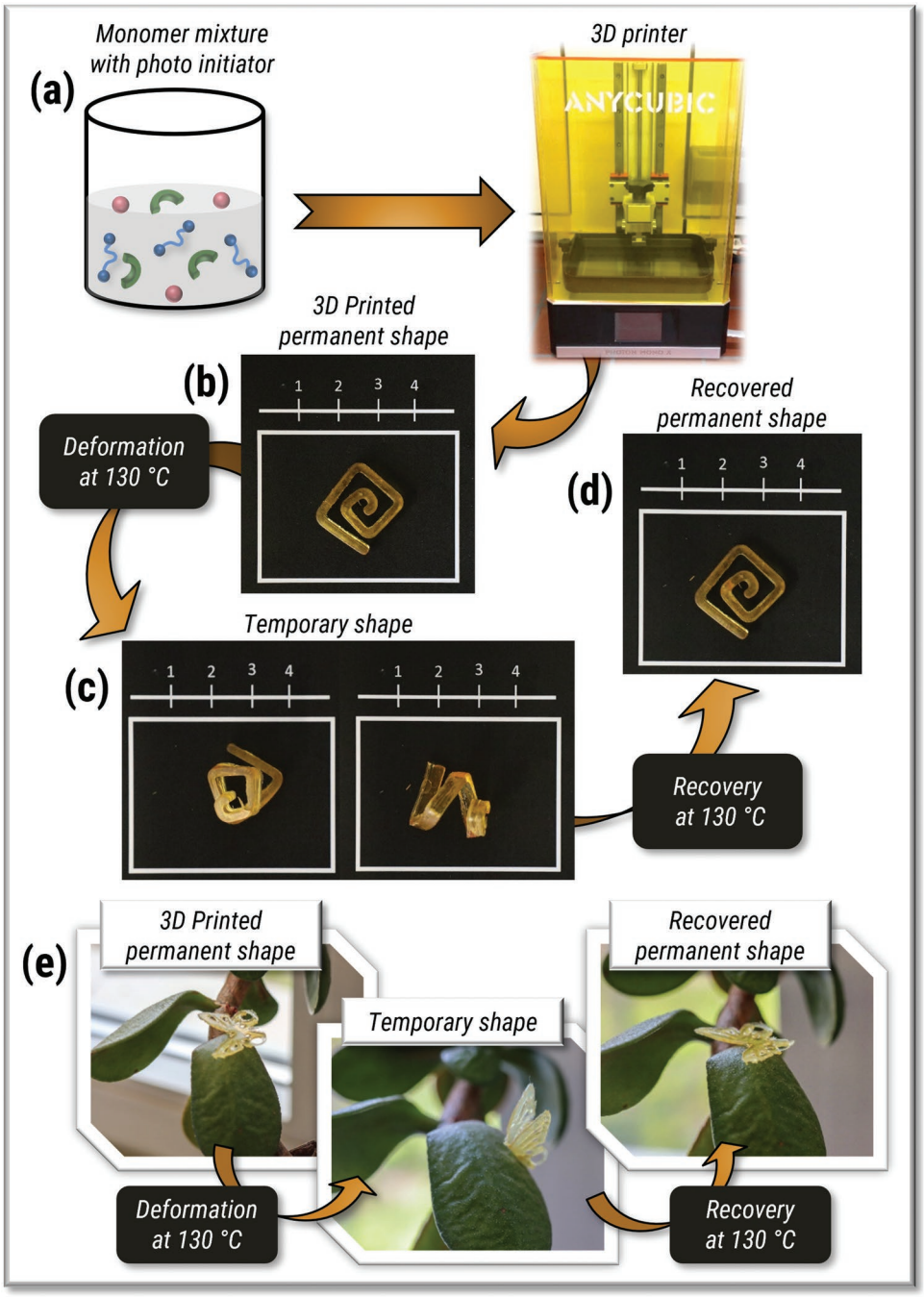

Figure 4. a) Schematic representation of the 3D-printed shape-memory polymer network $\mathbf{P_{3D}}$ containing reversible halogen bond interactions and photo series of one shape-memory cycle at a switching temperature of 130 °C (scale in cm), b) starting with the permanent shape, c) the fixed temporary shape and d) the recovery of the permanent shape and e) a photo series of the shape-memory test of a printed butterfly (size of butterfly ≈2 cm × 2 cm).

temperature of 70.2 °C was determined via DSC investigations (see Figure S54, Supporting Information). Furthermore, the TGA measurement revealed a high thermal stability with a degradation temperature of 268 °C (see Figure S55, Supporting Information). Those determined thermal properties are in a comparable temperature range with the values obtained for the polymers **P1** to **P3**. In order to quantify the shape-memory behavior, TMA investigations of the 3D-printed sample were performed. The resulting TMA plot is presented in Figure S56 (Supporting Information). The determined strain fixity rate of 93.5% is still very good; however, the value is a bit lower compared to the samples **P1** to **P3**.

This presumably results from the reduced amount of supramolecular cross-linking via the halogen bonds and, therefore, a lower content of switching units, which are responsible for the fixation of the temporary shape. For the recovery rate, a value

of 93.2% was determined, demonstrating a very good restorage of the original shape. Taking a closer look at the area of the recovery, it can also be observed in the TMA plot that $\mathbf{P_{3D}}$ is only able to recover the original shape well above the T_g. Thus, it can be concluded that, analogously to the samples **P1** to **P3** and **P1-I** to **P3-I**, the switching takes place via the activation of the reversible halogen bonds.

In order to exclude the possibility that hydrogen bonds are responsible for the fixation of the temporary shape, the deformed sample was placed in water in its temporary shape for 78 h (see Figure S59, Supporting Information). While an aqueous environment can induce the recovery step in the case of hydrogen bond-based SMPs (water-induced reversibility of the supramolecular bonds),[18] $\mathbf{P_{3D}}$ remained unchanged in the programmed temporary shape. This finding also shows another benefit of halogen bond-based polymers, since they feature a strong robustness against water.

3. Conclusion

In summary, we presented the synthesis of the first shape-memory polymer network based on halogen bond interactions. The formation of the supramolecular cross-linking was investigated via FT-Raman spectroscopy, isothermal titration calorimetry, and frequency dependent dynamic-mechanic analysis. Furthermore, the thermal properties of the polymers were investigated in a detailed fashion and several structure property relationships were obtained. The ITC investigations as well as the results of the FT-Raman spectroscopy and frequency sweep measurements revealed a stronger supramolecular interaction in the charged polymers **P1-I** to **P3-I** compared to the uncharged ones, in which the XB seems to be much weaker. Furthermore, it was found that the uncharged polymer networks **P1** to **P3** exhibit a higher degradation temperature while the glass transition temperature was mainly influenced by the content of the halogen bonds. Thermomechanical analyses revealed excellent shape-memory abilities for all presented samples with strain fixity rates above 95% and even strain recovery rates up to 99%. It turned out that the polymers **P1** and **P1-I** exhibited slightly better shape memory abilities compared to the **P2** and **P2-I**, which contain a higher content of XB. Furthermore, it was possible to associate the halogen bond with the shape-memory behavior of the materials and to exclude other supramolecular interactions, i.e., hydrogen bonds, as driving force for the shape-memory process. Finally, it was additionally possible to 3D-print a polymer bearing this supramolecular halogen bond cross-linking featuring the ability to recover the printed original shape within a few seconds at 130 °C. Moreover, the 3D-printed polymer is also stable against water treatment showing the high advantage of this type of material compared to hydrogen bond-based polymers.

4. Experimental Section

Detailed information about the synthesis and for the characterization methods are provided in the Supporting Information.

Supporting Information

Supporting Information is available from the Wiley Online Library or from the author.

Acknowledgements

J.M. and R.H.K. contributed equally to this work. The authors would like to thank the Deutsche Forschungsgemeinschaft (DFG, SCHU 1229/24-2, project number: 280016777 and CataLight subproject C2, project number: 364549901). Furthermore, the project was funded by the Carl-Zeiss Foundation (Perspektiven 2019).

Open access funding enabled and organized by Projekt DEAL.

Conflict of Interest

The authors declare no conflict of interest.

Data Availability Statement

The data that support the findings of this study are available in the supplementary material of this article.

Keywords

halogen bond interactions, shape-memory, smart materials, stimuli-responsive polymers

Received: June 27, 2022
Revised: August 7, 2022
Published online: September 4, 2022

[1] G. R. Desiraju, P. S. Ho, L. Kloo, A. C. Legon, R. Marquardt, P. Metrangolo, P. Politzer, G. Resnati, K. Rissanen, *Pure Appl. Chem.* **2013**, *85*, 1711.
[2] L. C. Gilday, S. W. Robinson, T. A. Barendt, M. J. Langton, B. R. Mullaney, P. D. Beer, *Chem. Rev.* **2015**, *115*, 7118.
[3] G. Cavallo, P. Metrangolo, R. Milani, T. Pilati, A. Priimagi, G. Resnati, G. Terraneo, *Chem. Rev.* **2016**, *116*, 2478.
[4] J. Y. C. Lim, P. D. Beer, *Chem. - Eur. J.* **2018**, *4*, 731.
[5] J. Pancholi, P. D. Beer, *Coord. Chem. Rev.* **2020**, *416*, 213281.
[6] A. Mukherjee, S. Tothadi, G. R. Desiraju, *Acc. Chem. Res.* **2014**, *47*, 2514.
[7] R. L. Sutar, S. M. Huber, *ACS Catal.* **2019**, *9*, 9622.
[8] D. Bulfield, S. M. Huber, *Chem. - Eur. J.* **2016**, *22*, 14434.
[9] R. Tepper, S. Bode, R. Geitner, M. Jäger, H. Görls, J. Vitz, B. Dietzek, M. Schmitt, J. Popp, M. D. Hager, U. S. Schubert, *Angew. Chem., Int. Ed.* **2017**, *56*, 4047.
[10] J. Dahlke, R. Tepper, R. Geitner, S. Zechel, J. Vitz, R. Kampes, J. Popp, M. D. Hager, U. S. Schubert, *Polym. Chem.* **2018**, *9*, 2193.
[11] R. Kampes, S. Zechel, M. D. Hager, U. S. Schubert, *Chem. Sci.* **2021**, *12*, 9275.
[12] M. D. Hager, S. Bode, C. Weber, U. S. Schubert, *Prog. Polym. Sci.* **2015**, *49–50*, 3.
[13] A. Lendlein, S. Kelch, *Angew. Chem., Int. Ed.* **2002**, *41*, 2034.
[14] C. Liu, H. Qin, P. T. Mather, *J. Mater. Chem.* **2007**, *17*, 1543.
[15] Y. Xia, Y. He, F. Zhang, Y. Liu, J. Leng, *Adv. Mater.* **2021**, *33*, 2000713.
[16] W. Zhang, H. Wang, H. Wang, J. Y. E. Chan, H. Liu, B. Zhang, Y.-F. Zhang, K. Agarwal, X. Yang, A. S. Ranganath, H. Y. Low, Q. Ge, J. K. W. Yang, *Nat. Commun.* **2021**, *12*, 112.

[17] A. Alteheld, Y. Feng, S. Kelch, A. Lendlein, *Angew. Chem., Int. Ed.* **2005**, *44*, 1188.
[18] M. Guo, L. M. Pitet, H. M. Wyss, M. Vos, P. Y. Dankers, E. W. Meijer, *J. Am. Chem. Soc.* **2014**, *136*, 6969.
[19] A. Lendlein, H. Jiang, O. Jünger, R. Langer, *Nature* **2005**, *434*, 879.
[20] Y. Guo, Z. Lv, Y. Huo, L. Sun, S. Chen, Z. Liu, C. He, X. Bi, X. Fan, Z. You, *J. Mater. Chem. B* **2019**, *7*, 123.
[21] B. K. Kim, S. Y. Lee, M. Xu, *Polymer* **1996**, *37*, 5781.
[22] A. Lendlein, A. M. Schmidt, M. Schroeter, R. Langer, *J. Polym. Sci. Part A: Polym. Chem.* **2005**, *43*, 1369.
[23] M. Ahmad, J. Luo, B. Xu, H. Purnawali, P. J. King, P. R. Chalker, Y. Fu, W. Huang, M. Miraftab, *Macromol. Chem. Phys.* **2011**, *212*, 592.
[24] G. Zhang, W. Peng, J. Wu, Q. Zhao, T. Xie, *Nat. Commun.* **2018**, *9*, 4002.
[25] J. Meurer, J. Hniopek, T. Bätz, S. Zechel, M. Enke, J. Vitz, M. Schmitt, J. Popp, M. D. Hager, U. S. Schubert, *Adv. Mater.* **2021**, *33*, 2006655.
[26] Q. Song, H. Chen, W. Yu, H. Ni, P. Hu, K. Zhao, *Mater. Today* **2019**, *16*, 1405.
[27] R. Dolog, R. A. Weiss, *Macromolecules* **2013**, *46*, 7845.
[28] T. Xie, *Nature* **2010**, *464*, 267.
[29] J. R. Kumpfer, S. J. Rowan, *JACS* **2011**, *133*, 12866.
[30] P. Zhang, M. Behl, X. Peng, M. Balk, A. Lendlein, *Chem. Mater.* **2019**, *31*, 5402.
[31] R. Tepper, B. Schulze, H. Görls, P. Bellstedt, M. Jäger, U. S. Schubert, *Org. Lett.* **2015**, *17*, 5740.
[32] B. R. Mullaney, B. E. Partridge, P. D. Beer, *Chem. - Eur. J.* **2015**, *21*, 1660.
[33] G. Cavallo, P. Metrangolo, T. Pilati, G. Resnati, M. Sansotera, G. Terraneo, *Chem. Soc. Rev.* **2010**, *39*, 3772.
[34] R. Wang, J. George, S. K. Potts, M. Kremer, R. Dronskowski, U. Englert, *Acta Cryst. C* **2019**, *75*, 1190.
[35] M. T. Messina, P. Metrangolo, W. Navarrini, S. Radice, G. Resnati, G. Zerbi, *J. Mol. Struct.* **2000**, *524*, 87.
[36] S. V. Rosokha, C. L. Stern, J. T. Ritzert, *Chem. - Eur. J.* **2013**, *19*, 8774.
[37] J. Lieffrig, O. Jeannin, A. Frąckowiak, I. Olejniczak, R. Świetlik, S. Dahaoui, E. Aubert, E. Espinosa, P. Auban-Senzier, M. Fourmigué, *Chem. - Eur. J.* **2013**, *19*, 14804.
[38] A. Eisenberg, B. Hird, R. B. Moore, *Macromolecules* **2002**, *23*, 4098.
[39] J. Dahlke, R. K. Bose, S. Zechel, S. J. Garcia, S. van der Zwaag, M. D. Hager, U. S. Schubert, *Macromol. Chem. Phys.* **2017**, *218*, 1700340.
[40] R. K. Bose, N. Hohlbein, S. J. Garcia, A. M. Schmidt, S. van der Zwaag, *Phys. Chem. Chem. Phys.* **2015**, *17*, 1697.
[41] T. Aida, E. W. Meijer, S. I. Stupp, *Science* **2021**, *335*, 813.
[42] F. Gamardella, F. Guerrero, S. De la Flor, X. Ramis, A. Serra, *Europ. Polym. J.* **2020**, *122*, 109361.
[43] K. Yu, P. Taynton, W. Zhang, M. L. Dunn, H. J. Qi, *RSC Adv.* **2014**, *4*, 10108.
[44] S. Götz, M. Abend, S. Zechel, M. D. Hager, U. S. Schubert, *J. Appl. Polym. Sci.* **2019**, *136*, 47064.
[45] S. Bode, R. K. Bose, S. Matthes, M. Ehrhardt, A. Seifert, F. H. Schacher, R. M. Paulus, S. Stumpf, B. Sandmann, J. Vitz, A. Winter, S. Hoeppener, S. J. Garcia, S. Spange, S. van der Zwaag, M. D. Hager, U. S. Schubert, *Polym. Chem.* **2013**, *4*, 4966.
[46] S. Chen, W. H. Binder, *Acc. Chem. Res.* **2016**, *49*, 1409.
[47] S. Chen, D. Döhler, W. H. Binder, *Polymer* **2016**, *107*, 466.
[48] A. Eisenberg, B. Hird, R. B. Moore, *Macromolecules* **1990**, *23*, 4098.
[49] F. Herbst, S. Seiffert, W. H. Binder, *Polym. Chem.* **2012**, *3*, 3084.
[50] F. Herbst, K. Schröter, I. Gunkel, S. Gröger, T. Thurn-Albrecht, J. Balbach, W. H. Binder, *Macromolecules* **2010**, *43*, 10006.
[51] C. L. Lewis, K. Stewart, M. Anthamatten, *Macromolecules* **2014**, *47*, 729.
[52] H. Rupp, W. H. Binder, *Front. Chem.* **2021**, *9*, 771974.
[53] G. Ehrmann, A. Ehrmann, *J. Appl. Polym. Sci.* **2021**, *138*, 50847.
[54] J. Zhang, Z. Yin, L. Ren, Q. Liu, L. Ren, X. Yang, X. Zhou, *Adv. Mater. Technol.* **2022**, 2101568, https://doi.org/10.1002/admt.202101568.
[55] C. A. Spiegel, M. Hackner, V. P. Bothe, J. P. Spatz, E. Blasco, *Adv. Funct. Mater.* **2022**, 2110580, https://doi.org/10.1002/adfm.202110580.
[56] B. Steyrer, P. Neubauer, R. Liska, J. Stampfl, *Materials* **2017**, *10*, 1445.